Interpreting Visibility Amplitudes

Christian A. Hummel (European Southern Observatory)

Acknowledgements: Michelson Summer School Authors

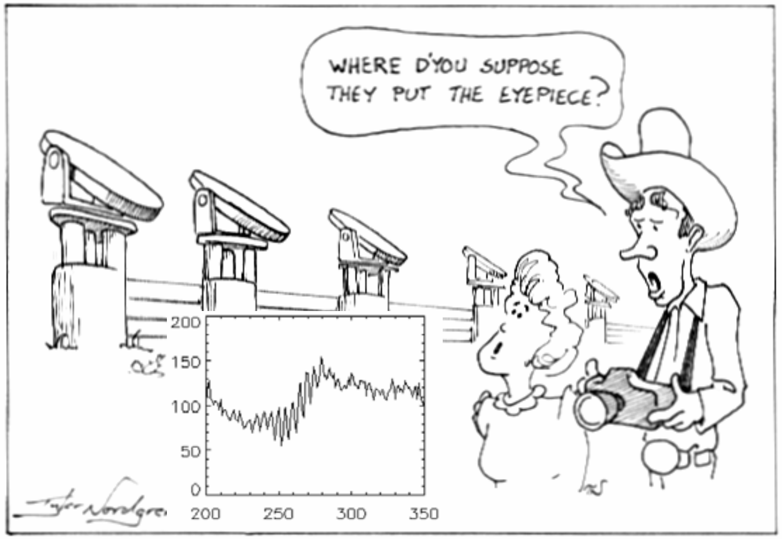

Courtesy of Tyler Nordgren

Overview

- Interferometers as telescopes
- Responses to simple models
- Aperture plane visibility
- Example interpretations
- Polychromatic interferometry
- Extended sources
- Not enough data?

Interferometers as telescopes

- Photometric field of view
- Interferometric field of view
- Aperture synthesis
- Sensitivity: it’s the correlated flux!

Photometric field of view

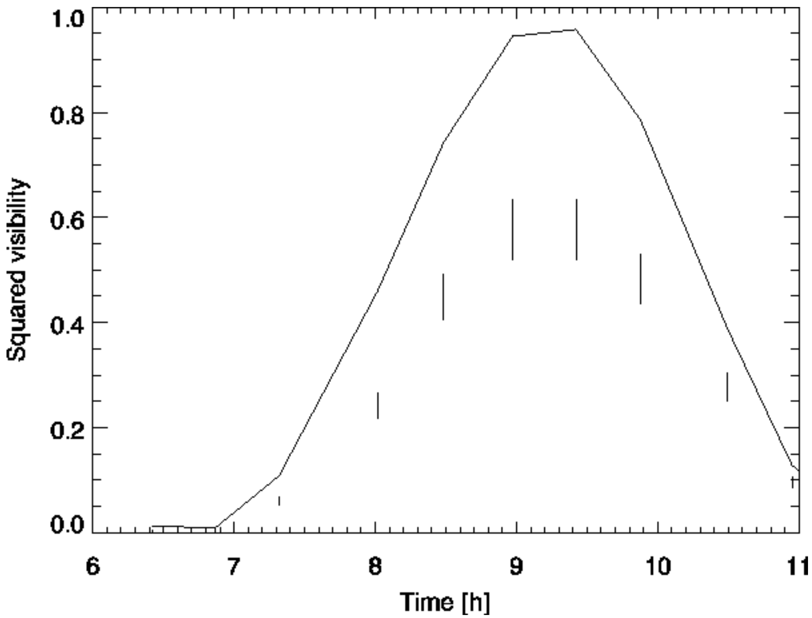

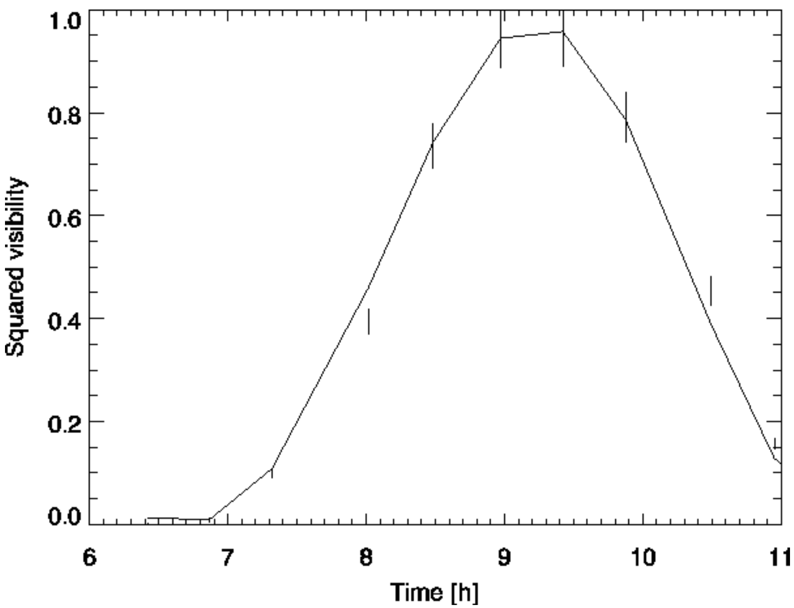

Mizar A (V=2.3)
with B (V=4.0) at 14”
(Mark III)

$$f = (1 + 10^{-\Delta m/2.5})^2$$

Interferometric field of view (I)

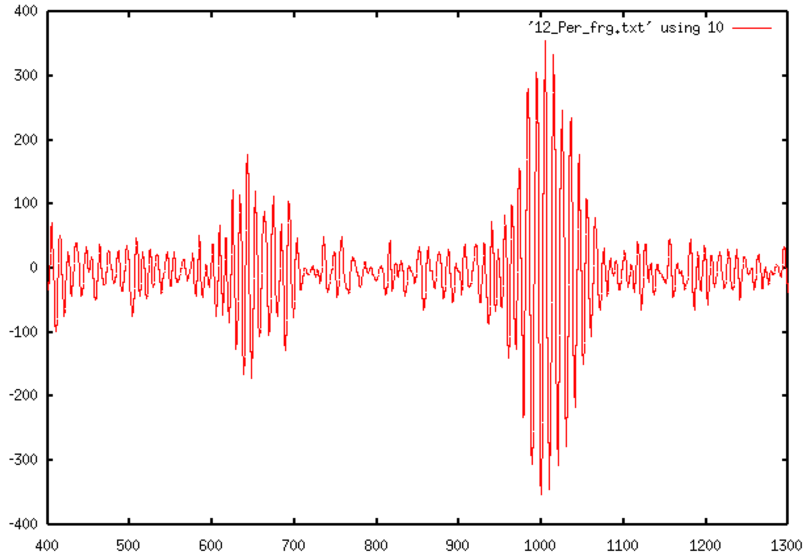

12 Persei observed on Oct 9, 2001 with the CHARA Array, K'-band, 330m baseline, separation 40 marcsec

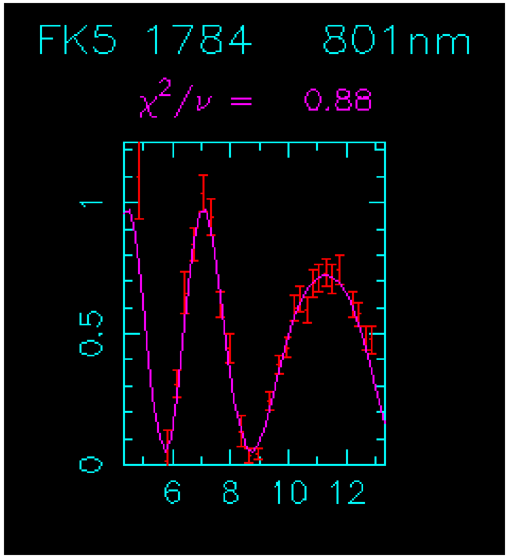

Mark 3 (Oct 8, 1992)

Interferometric field of view (II)

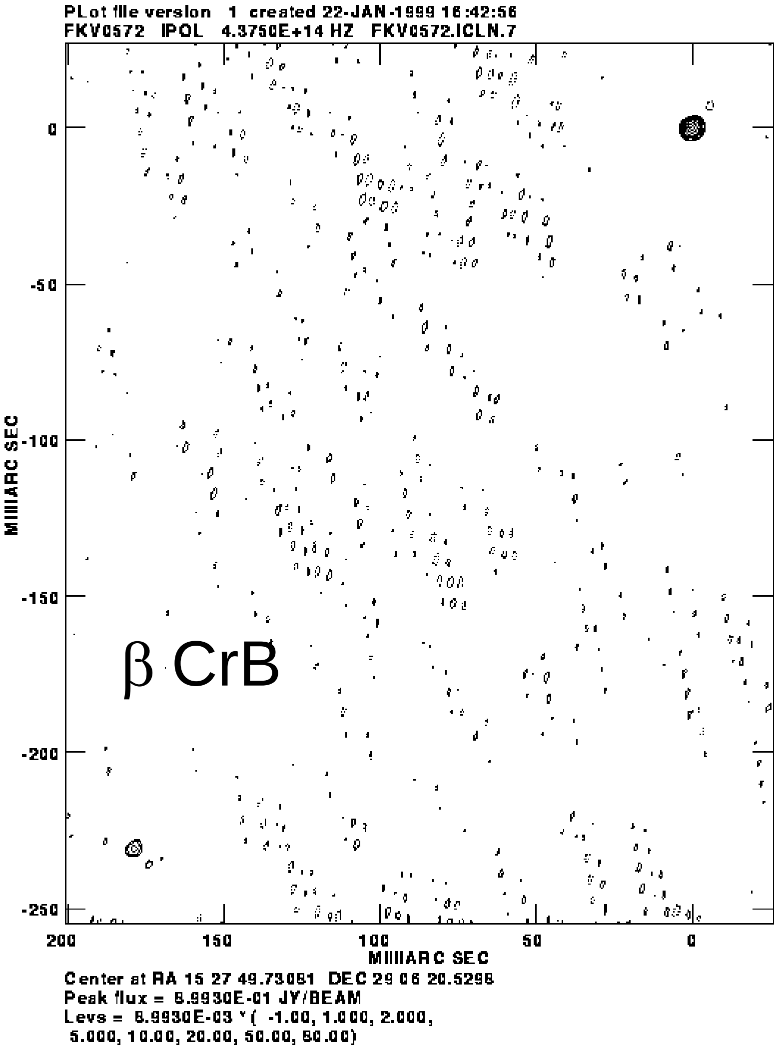

β CrB

$$\Delta\alpha = R\frac{\lambda}{B}$$

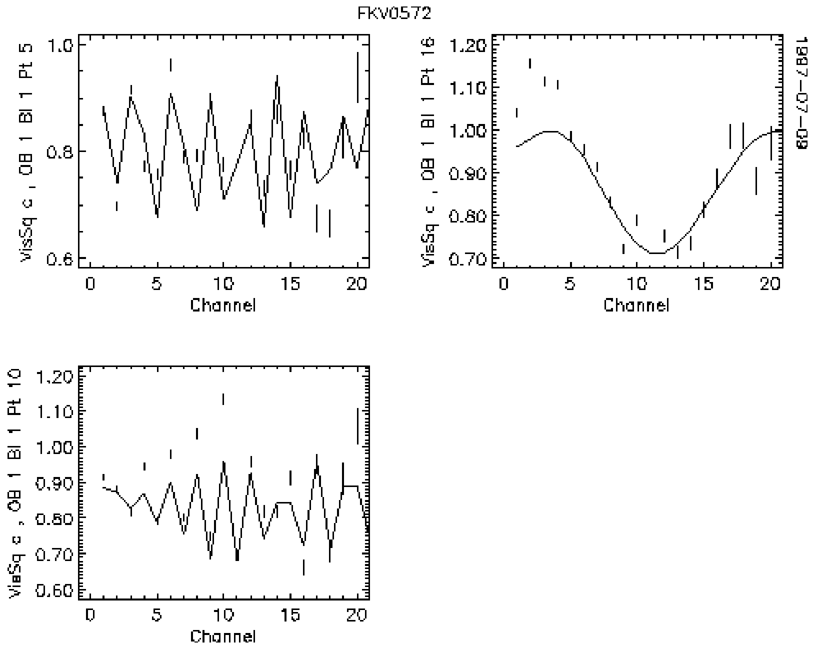

(NPOI)

Aperture synthesis

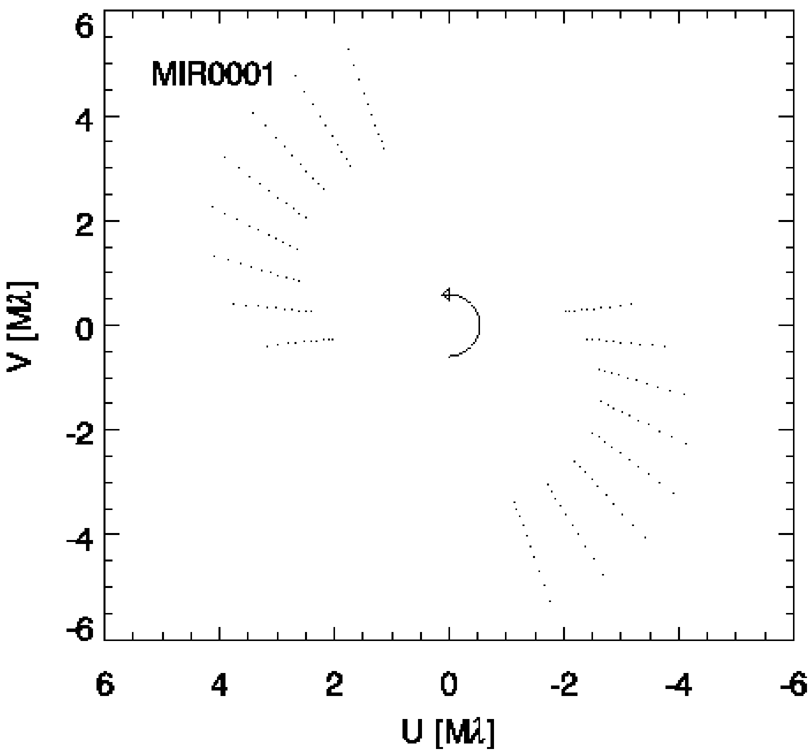


```
function mapvis,map,u,v
;
; Compute the visibility for a map at a single coordinate u and v[lambda].
; Map positions are in mas. map.x corresponds to RA and increases towards
; East, i.e. left.
;
RAD=180/!pi
MAS=1/3600000.d0
;
arg=2*!pi*(u*map.x+v*map.y)*MAS/RAD
;
return,total(map.i*complex(cos(arg),sin(arg)))
;
end
                                                  1,1           Top
```

MIDI, UT2-UT3, $\delta = -61$

Aperture synthesis and orbital motion

β Aur
(Mark III)

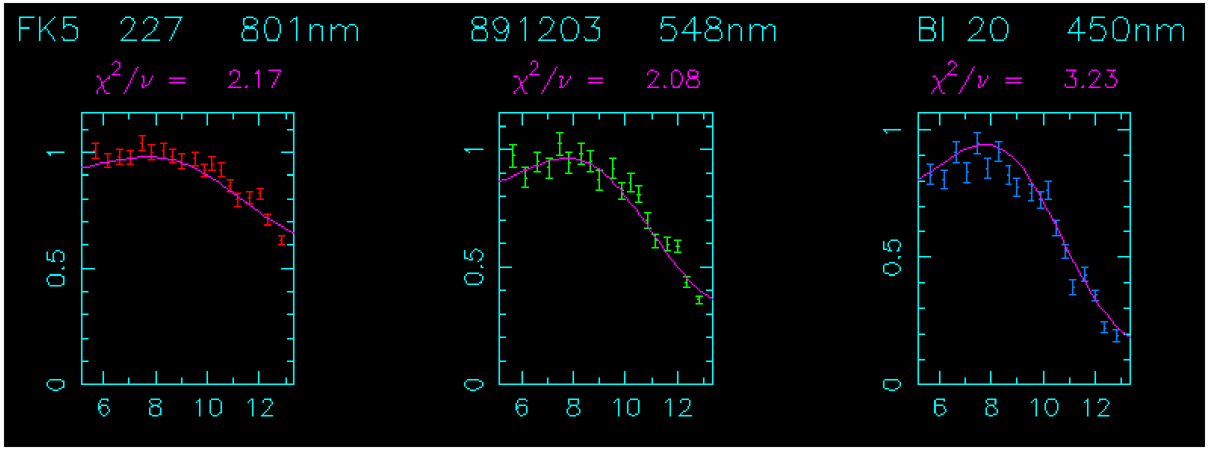

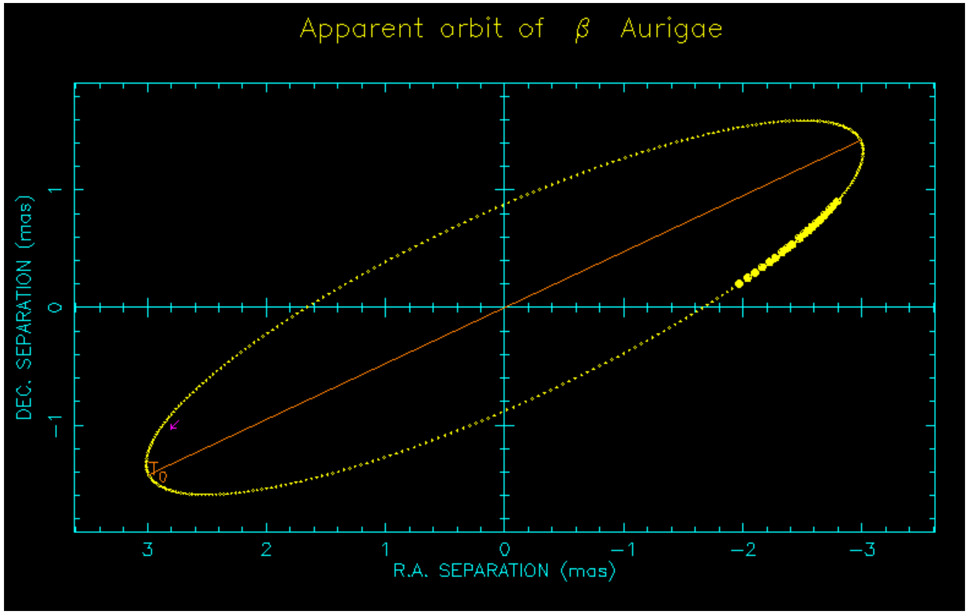

P = 4 days

Responses to simple models

- Point source (“unresolved”)
- Uniform disk
- Elliptical disk
- Limb darkened disk
- Gaussian
- Binary, mystery star
- Ring

Uniform disk

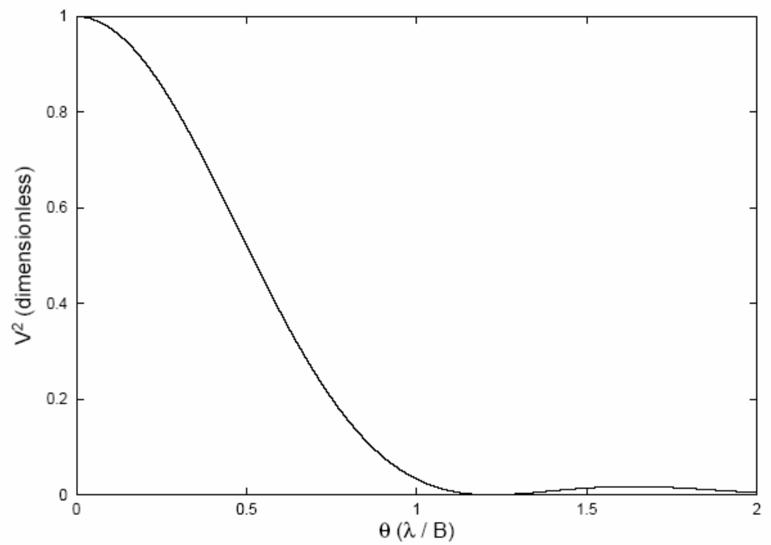

Figure 2.6: Squared Normalized Visibility Amplitude for the Uniform Disk. The disk diameter θ is plotted in units of the interferometer fringe spacing $\lambda / B_{\perp}$.

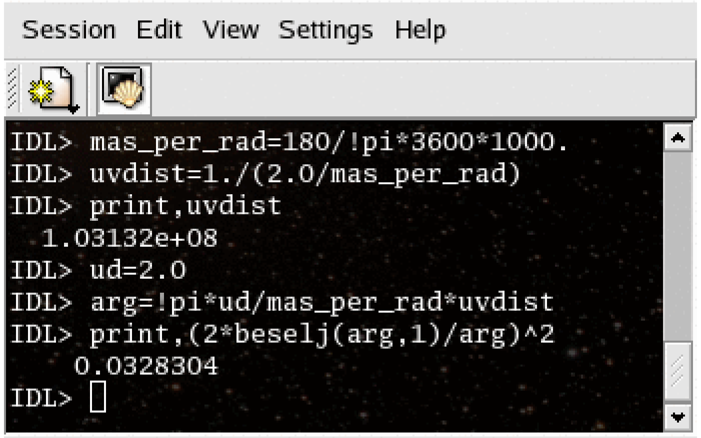

Elliptical disk

```
u_r=            v*cos(disk.pa)+u*sin(disk.pa)
v_r=disk.ratio*(u*cos(disk.pa)-v*sin(disk.pa))
```

Transform (u,v) coord.

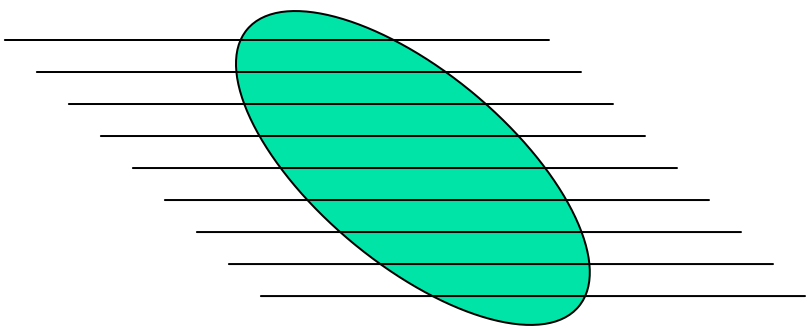

Fourier transform strip brightness distribution

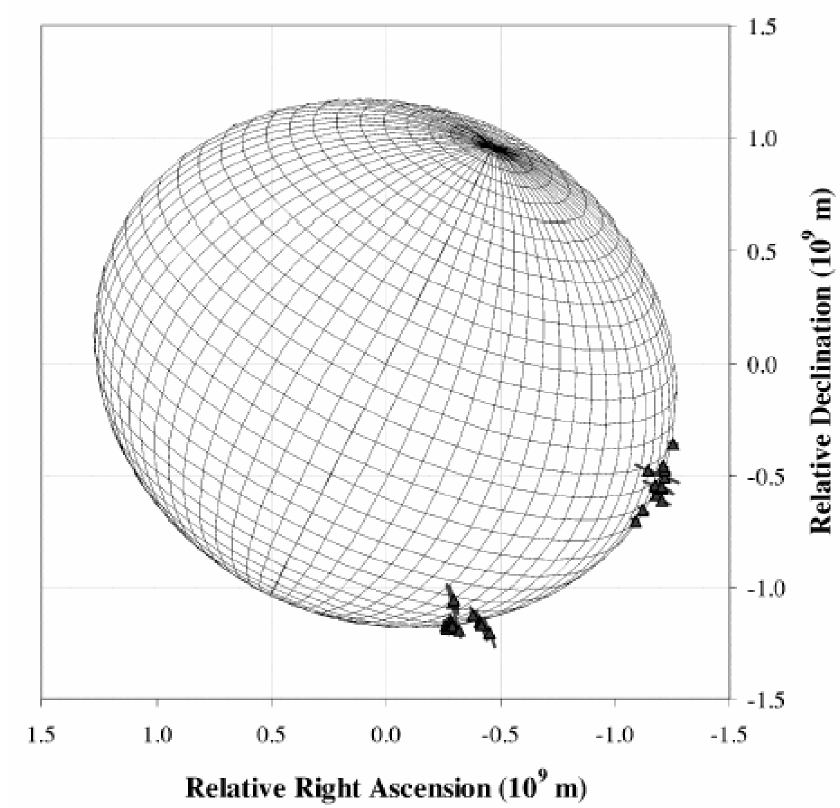

van Belle et al. (2001)

Limb darkened disk

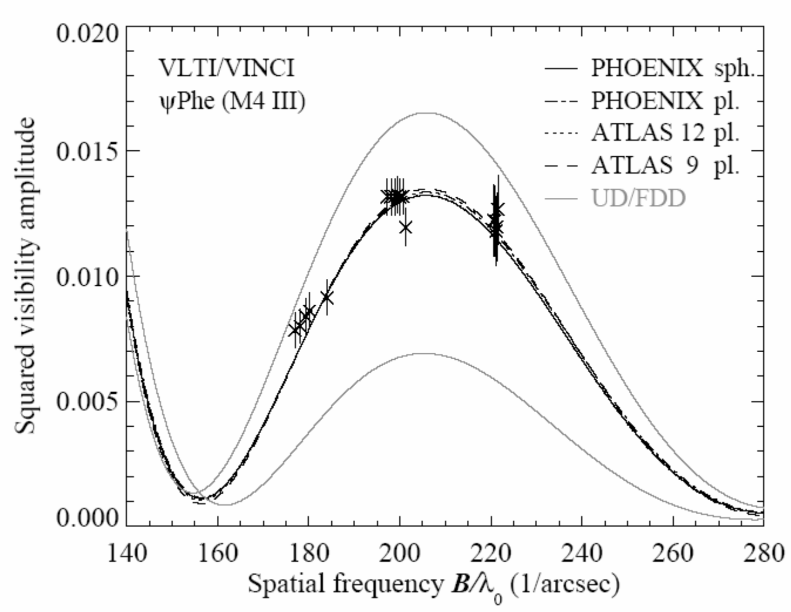

Wittkowski et al. (2003)

$$D_\lambda(\mu)=I_\lambda(\mu)/I_\lambda(1)=1-x_\lambda(1-\mu).$$

```
alpha=1-ld_coeffs
beeta=ld_coeffs
arg=!pi*model.diameter*mas2rad*sqrt(u^2+v^2)
visamp=(alpha*beselj(arg,1)/arg+beeta*sqrt(!pi/2)* $
        sqrt(2/(!pi*arg))*(sin(arg)/arg-cos(arg))/ $
        sqrt(arg*arg*arg))/(alpha/2+beeta/3)
return,complex(visamp)*flux
```

Binary

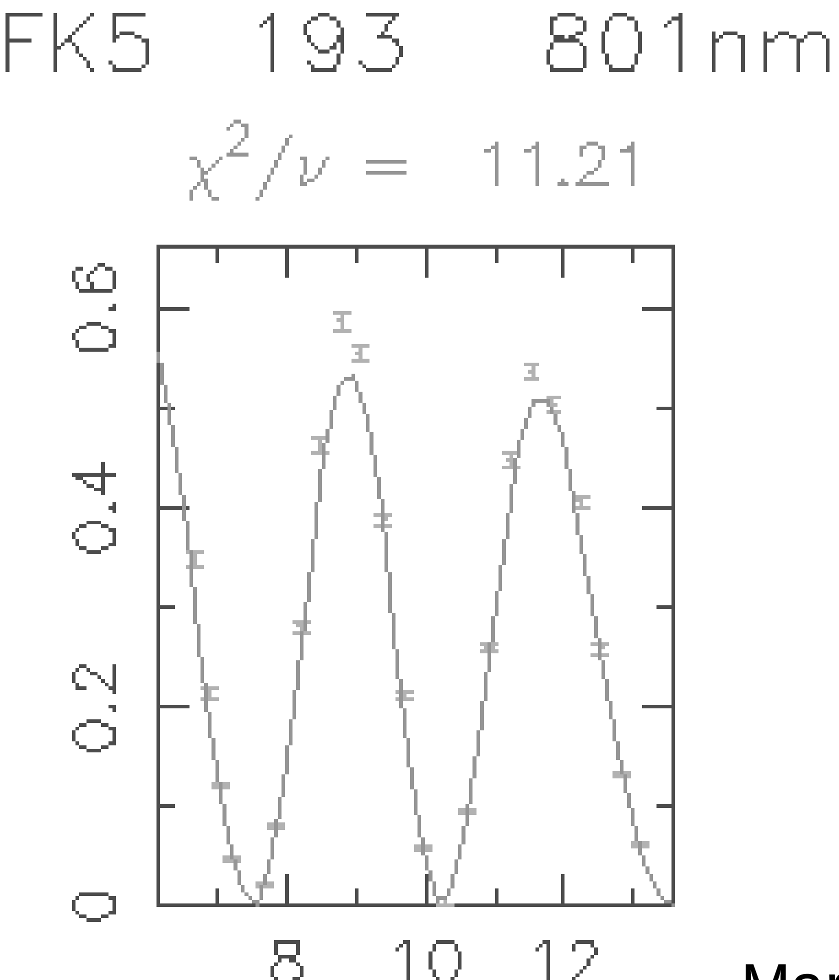

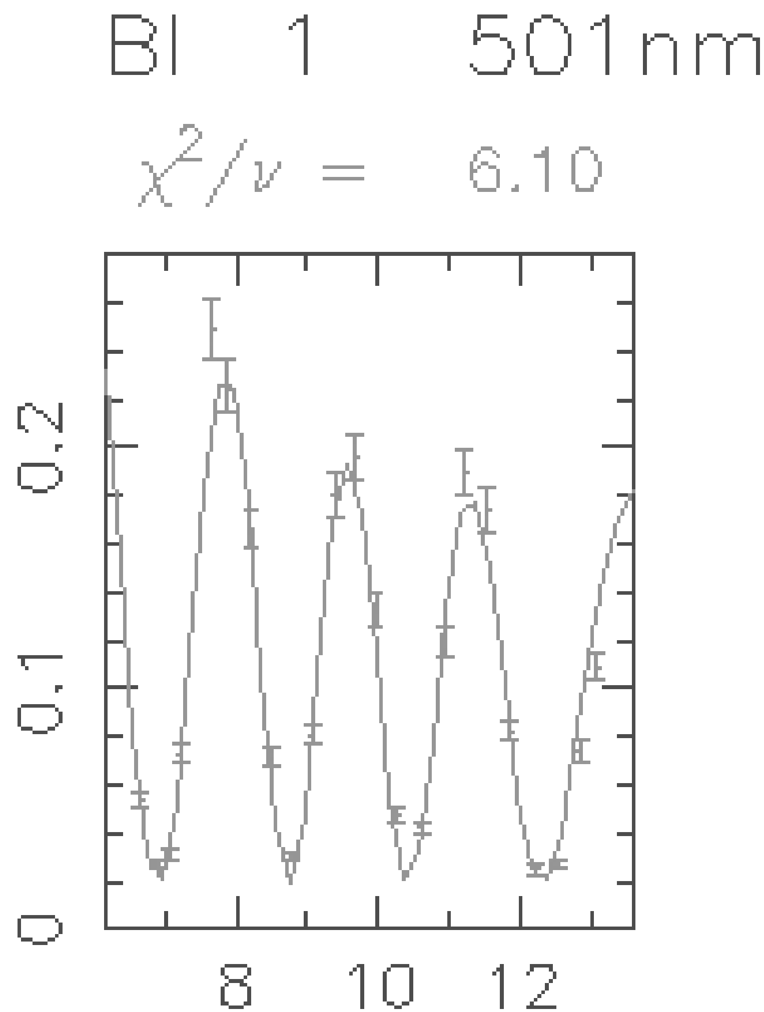

Mark III

How to estimate PA and separation

Capella with the Mark III

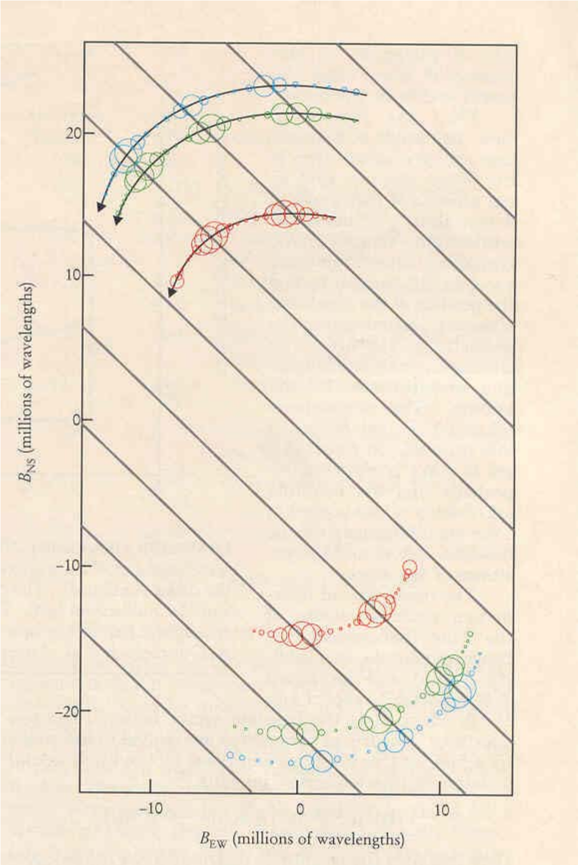

Armstrong et al. 1995

Mystery star

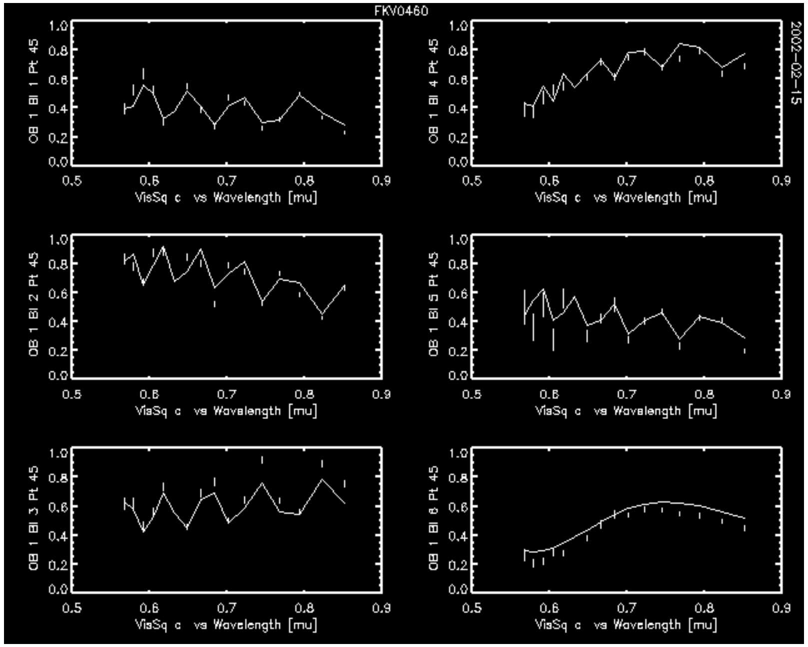

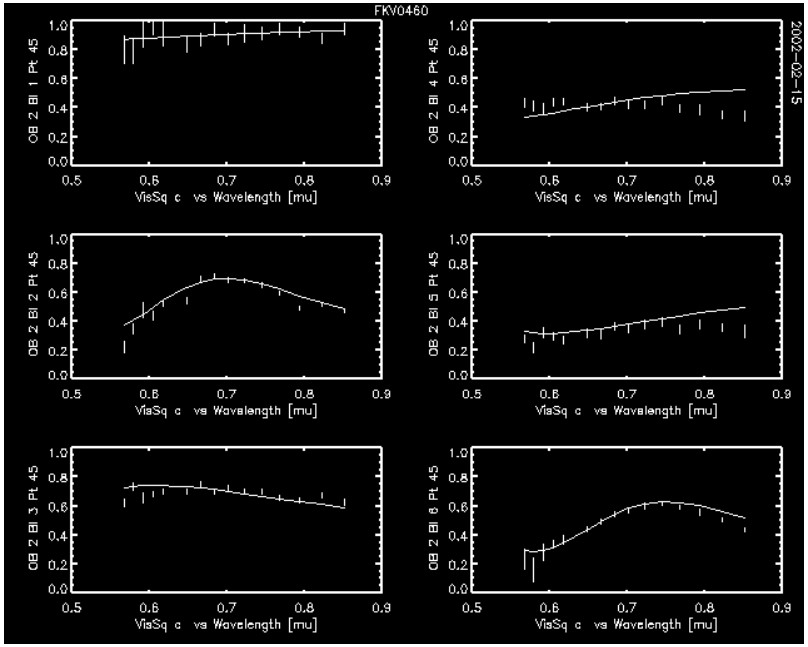

All baseline PAs

2nd spectr., One PA

Triple star

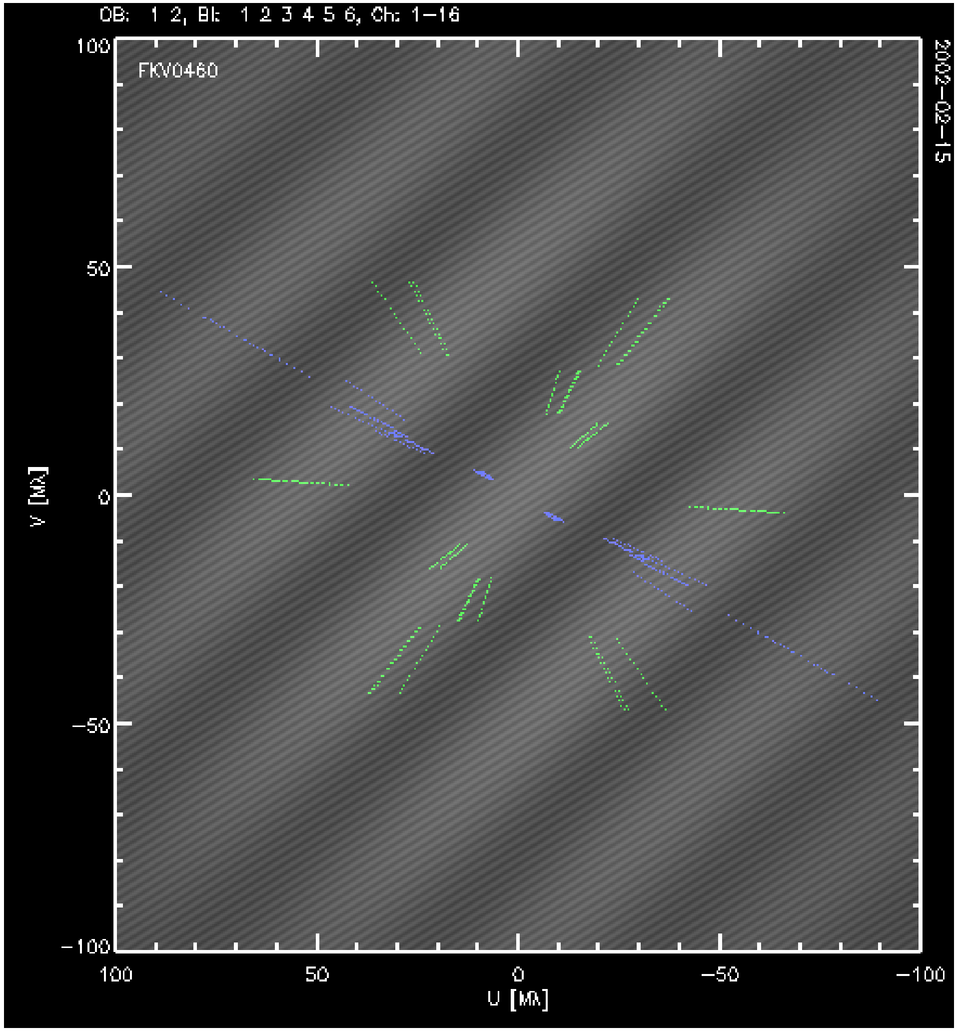

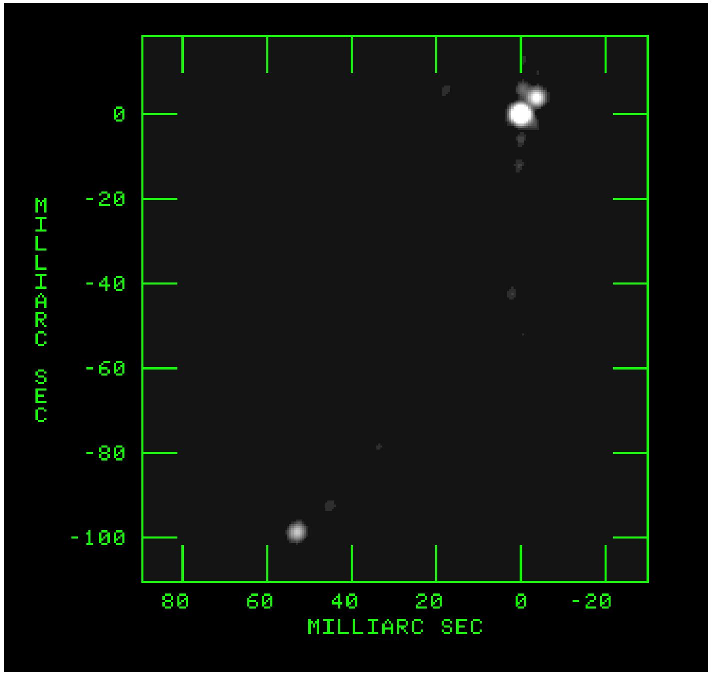

η Vir (Hummel et al. 2004)

Aperture plane visibility

- Equal magnitude binary
- Resolved component in binary
- Faint secondary vs resolved primary
- Archimedes spiral

Equal magnitude binary

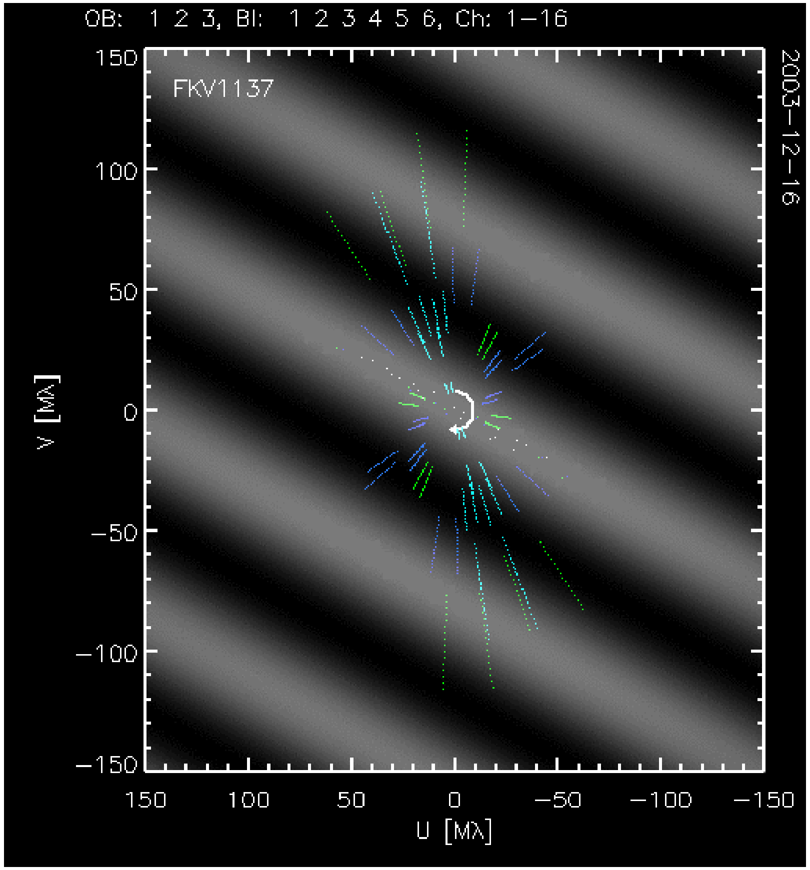

Resolved component in binary

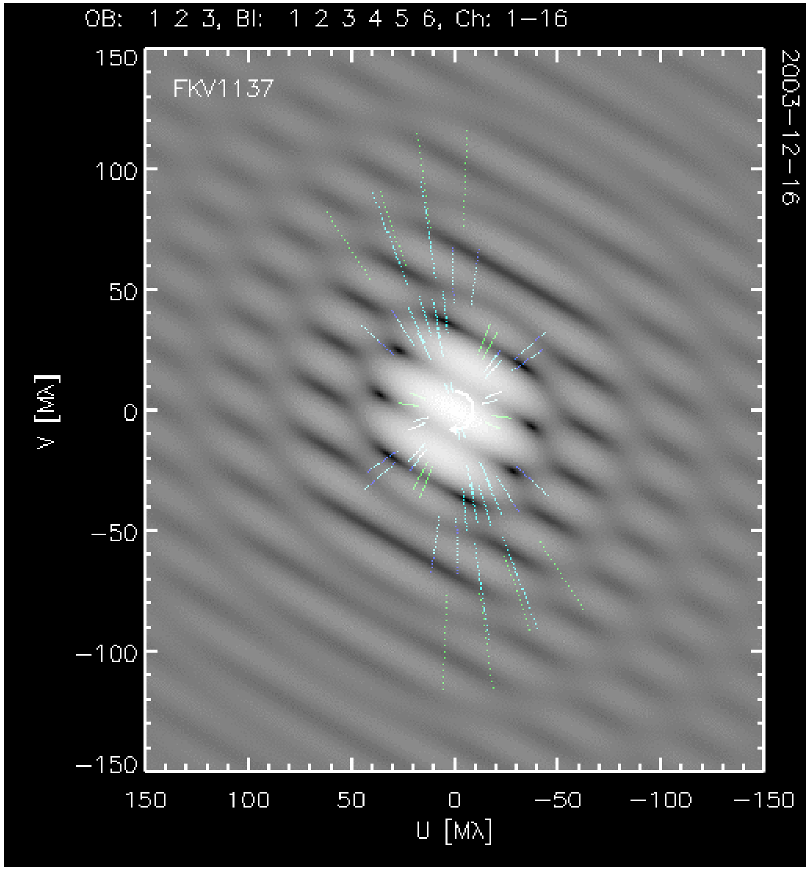

Faint secondary vs resolved primary

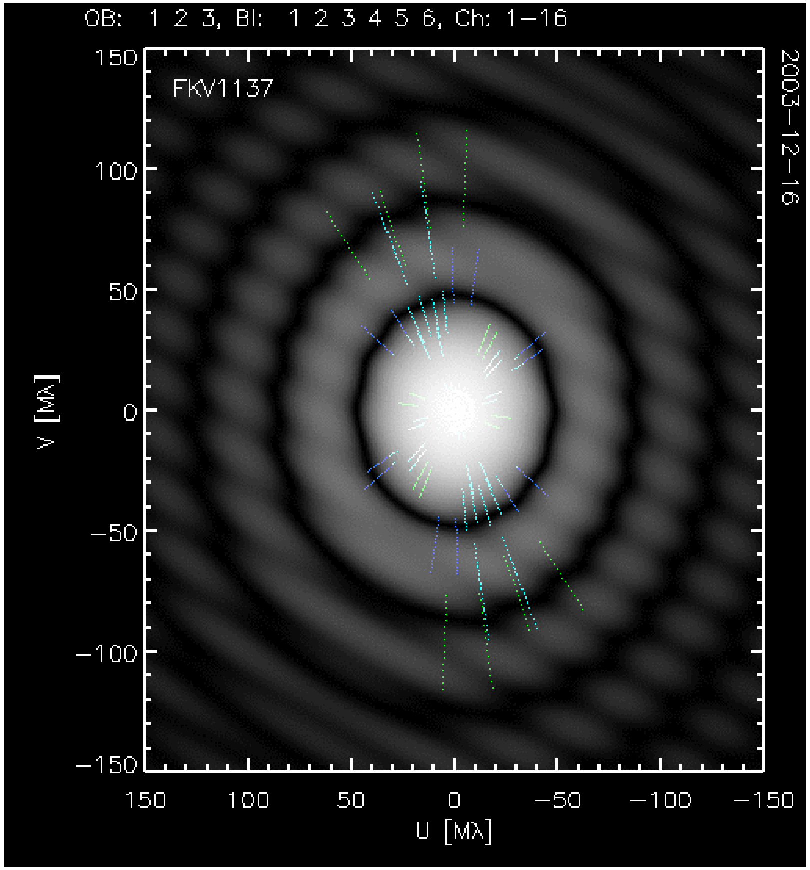

Archimedes spiral

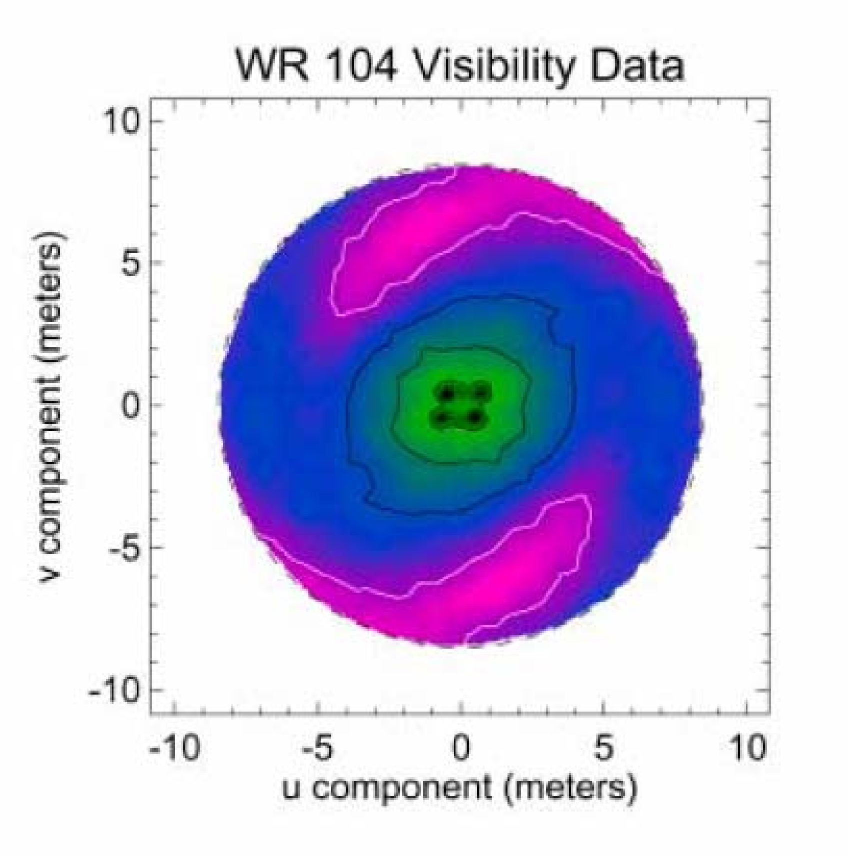

Monnier et al. 1999

Example interpretations (1)

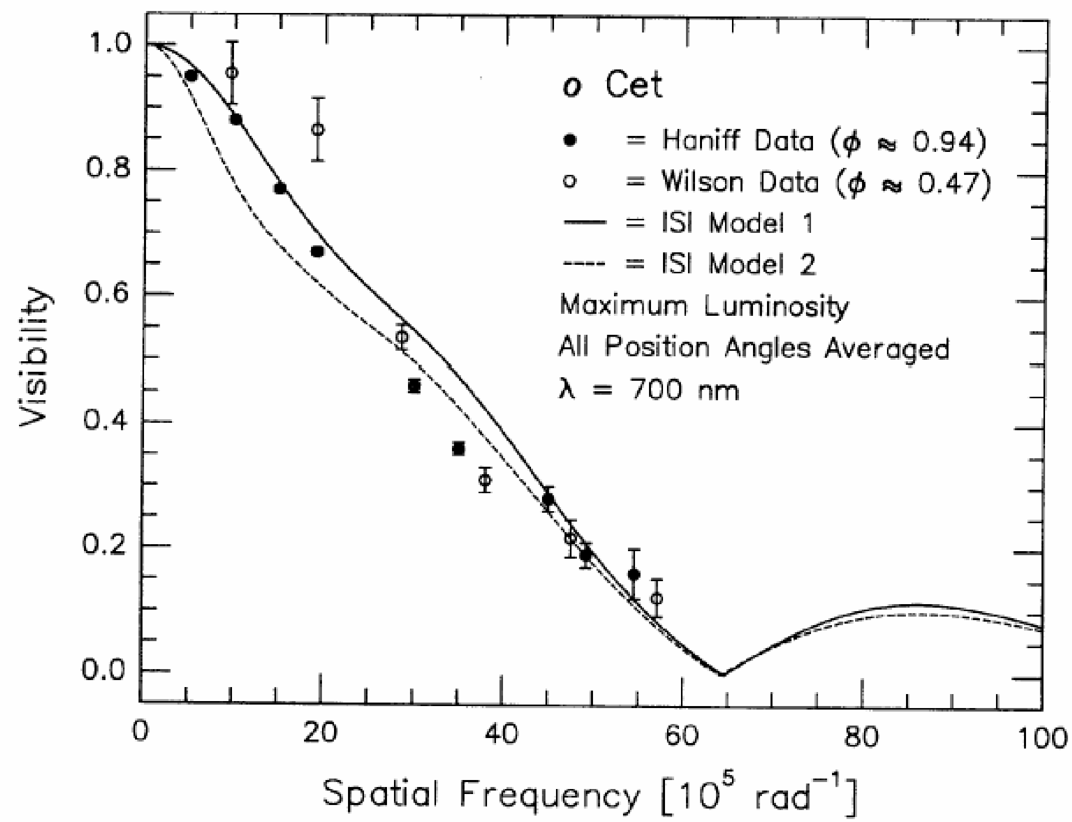

Danchi et al. 1994

Example interpretations (2)

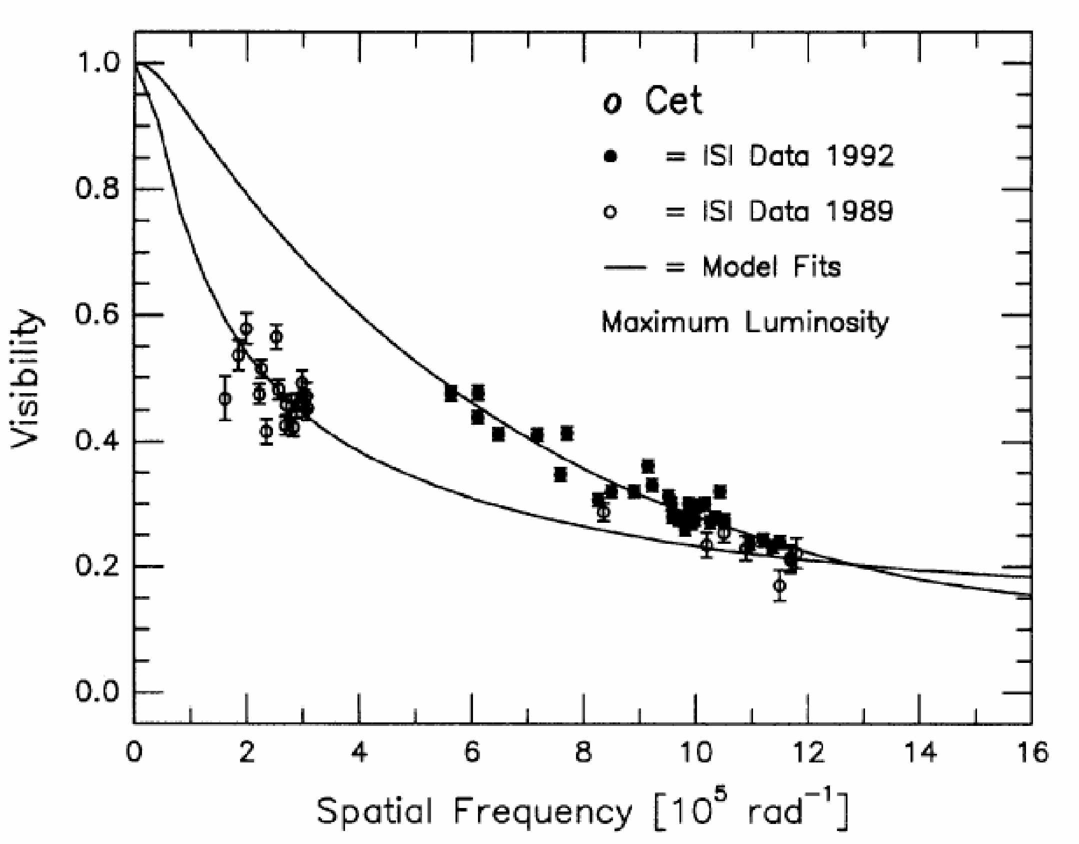

Danchi et al. 1994

Example interpretations (3)

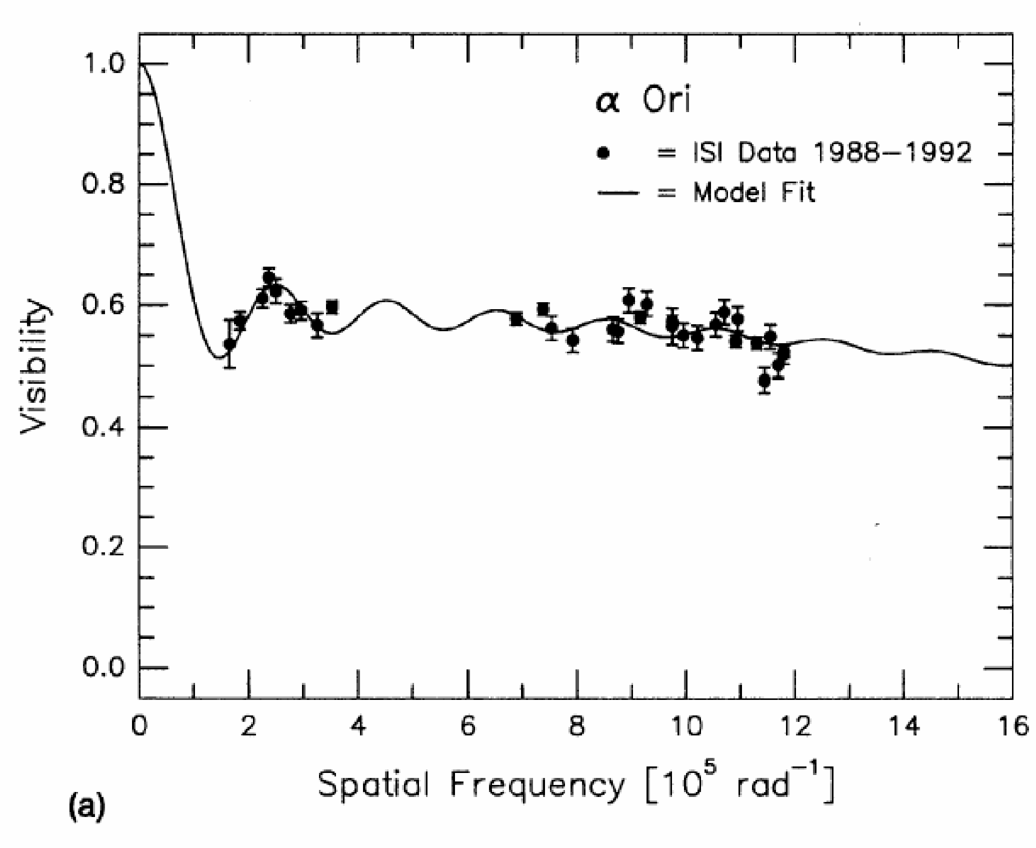

Danchi et al. 1994

Example interpretations (4)

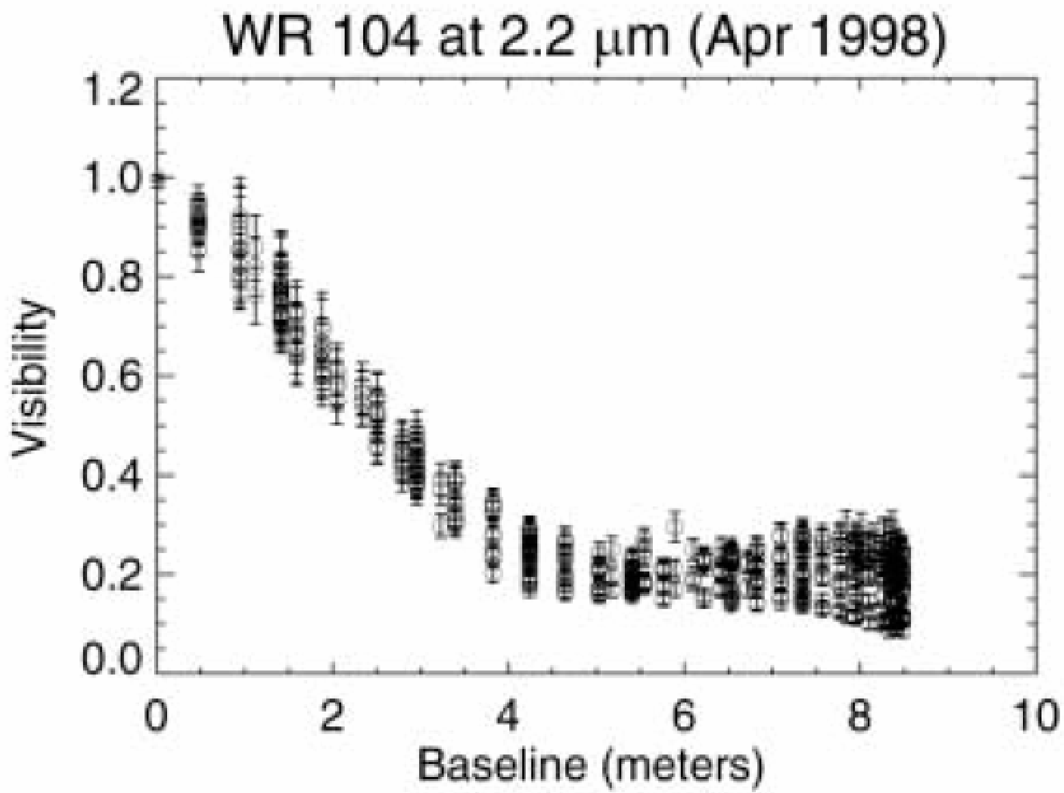

Monnier et al. 1999

Example interpretations (5a)

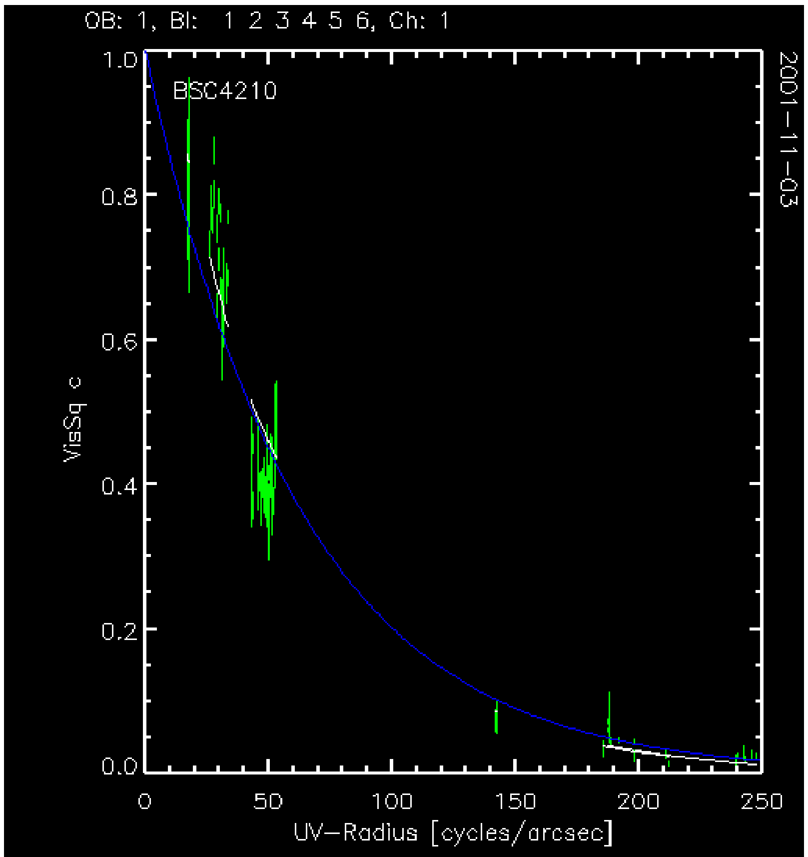

VLTI/VINCI

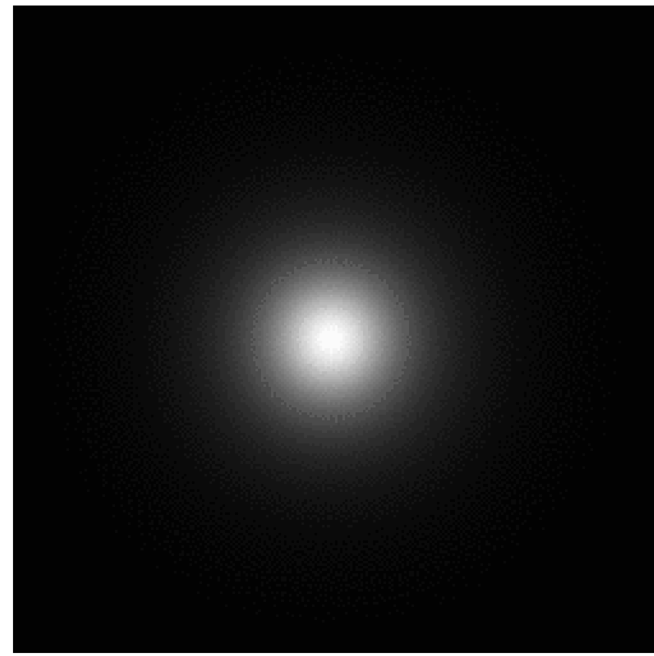

```
function pearson_funct,x,a
;
return,a(0)/(1.+((2.*x*sqrt(2.^(1./a(1))-1))/a(2))^2)^a(1)
;
end
```

η Car

Example interpretations (5b)

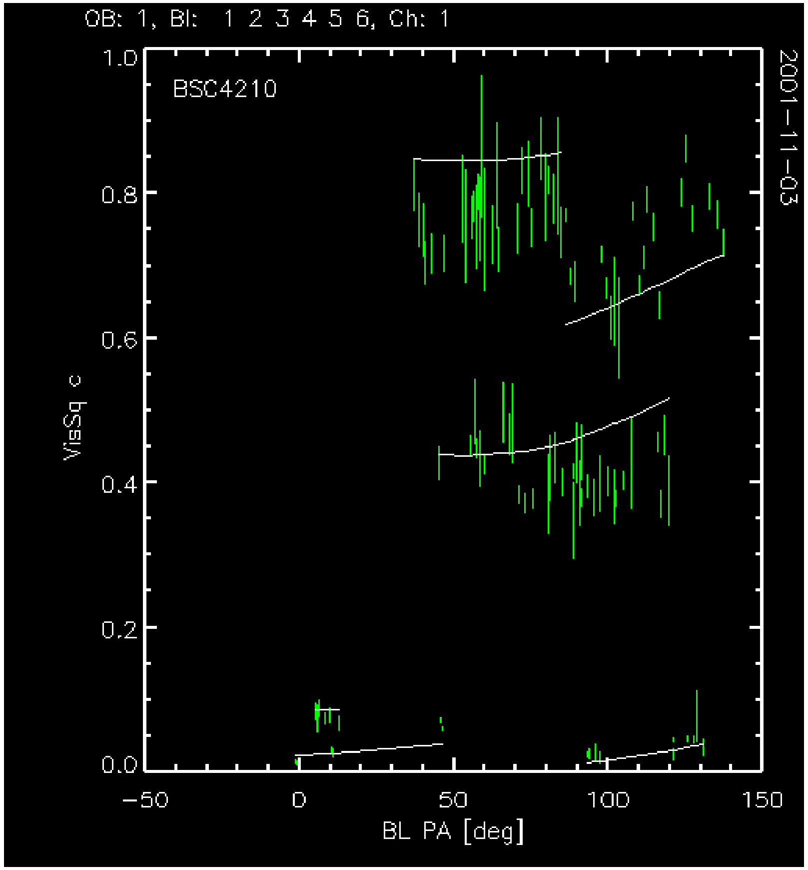

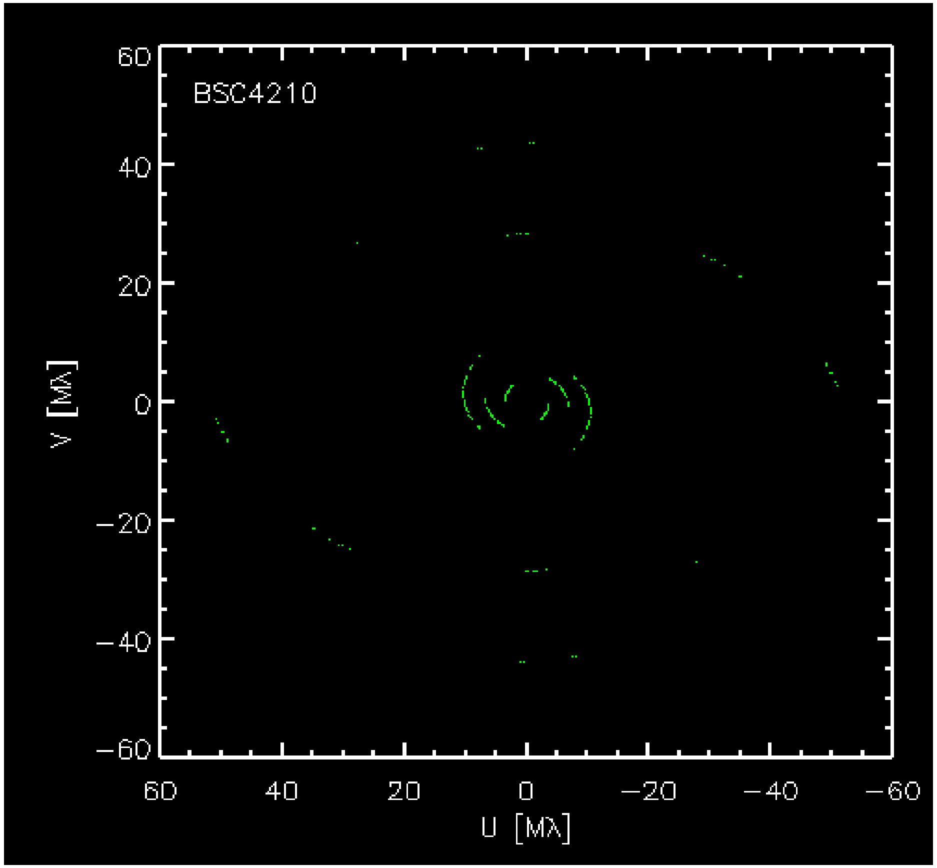

VLTI/VINCI

Polychromatic interferometry

- Disperse the light!
- Broad band aperture synthesis
- Source structure dependent on wavelength

Composite spectrum binary

η Peg
(NPOI)

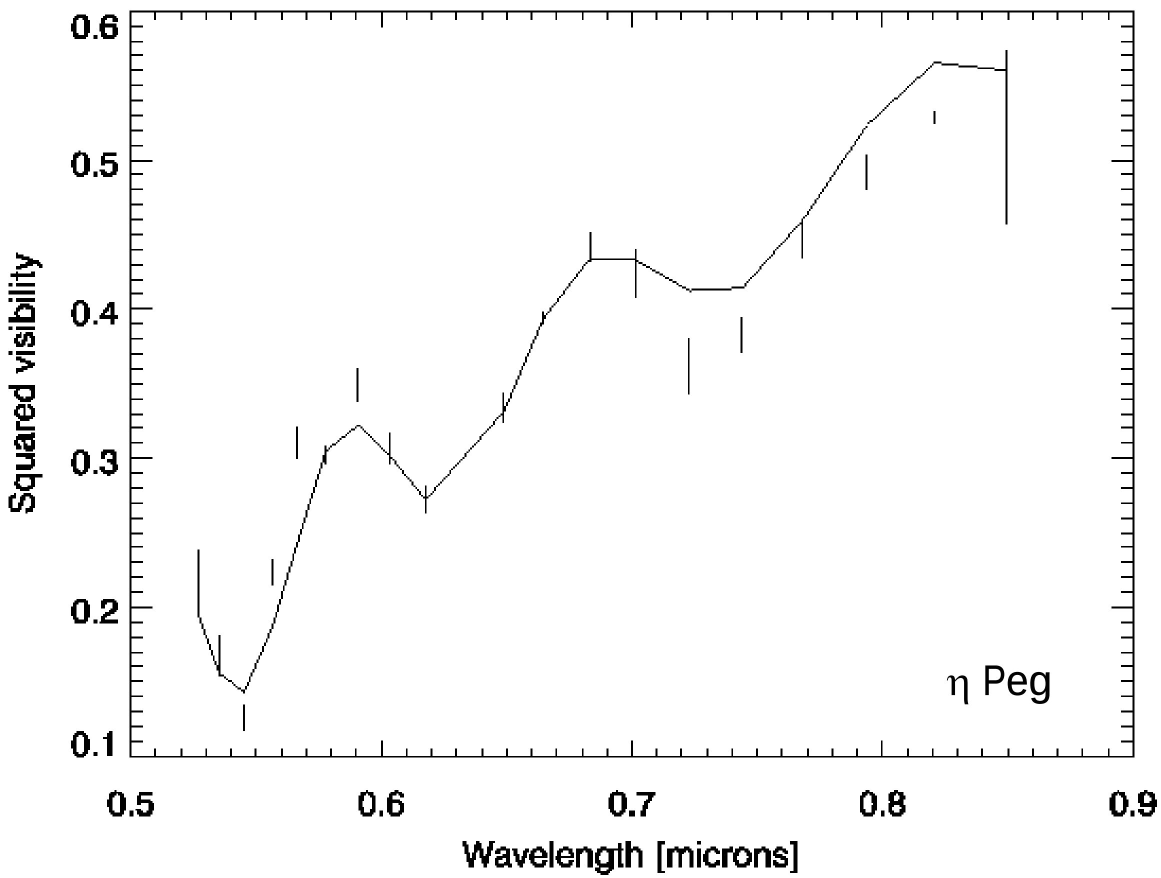

Stellar atmospheres

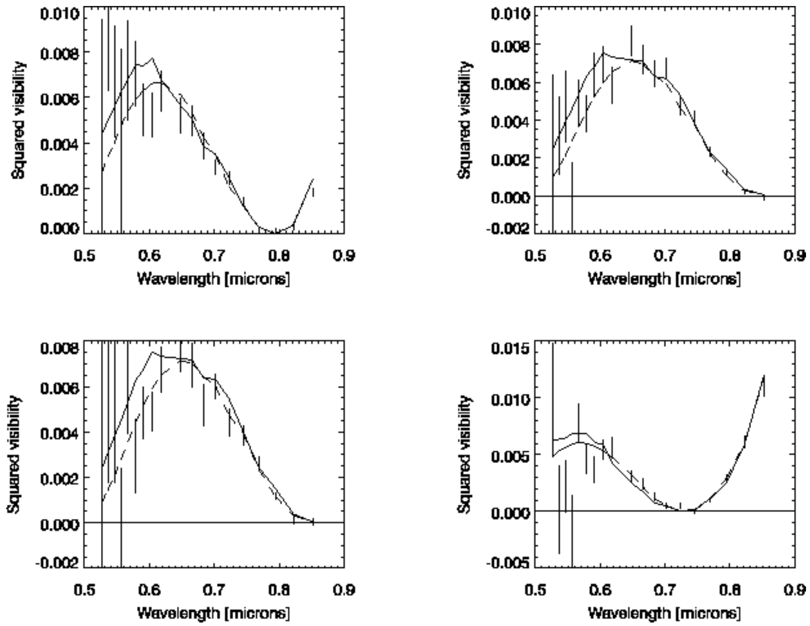

$$V_{\mathrm{LD}}(\lambda) = \int_0^1 S_\lambda I_\lambda^\mu J_0[\pi\,\theta_{\mathrm{LD}}\,(B/\lambda)\,(1-\mu^2)^{1/2}]\,\mu\,d\mu$$

```
f1=(mu*profile)/profile(n_elements(mu)-1)
f2=beselj(arg*sqrt(1-mu^2),0)*f1
;
return,int_tabulated(mu,f2)/int_tabulated(mu,f1)
```

γ Sge

MIDI visibility spectra of disks

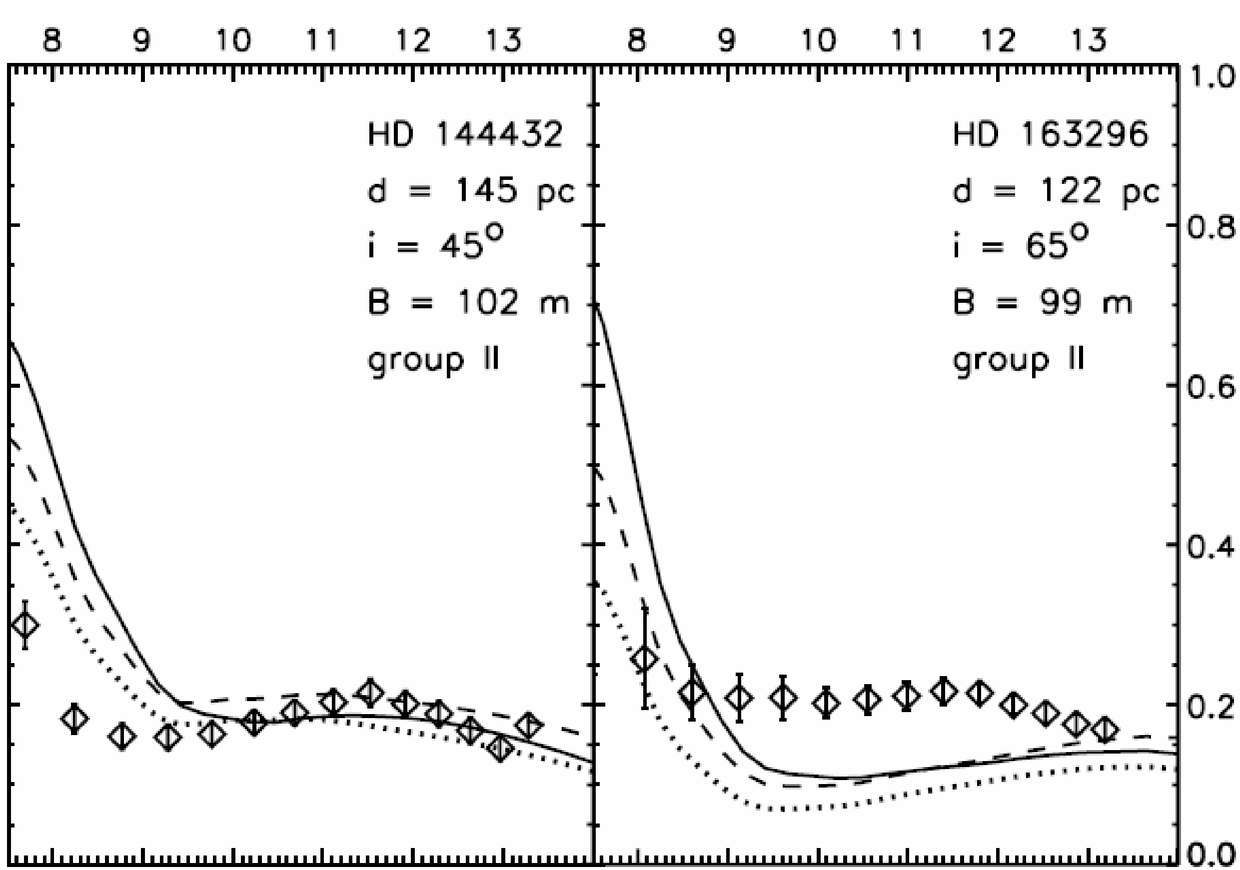

Leinert et al. 2004

NGC 1068 arcsecond scales

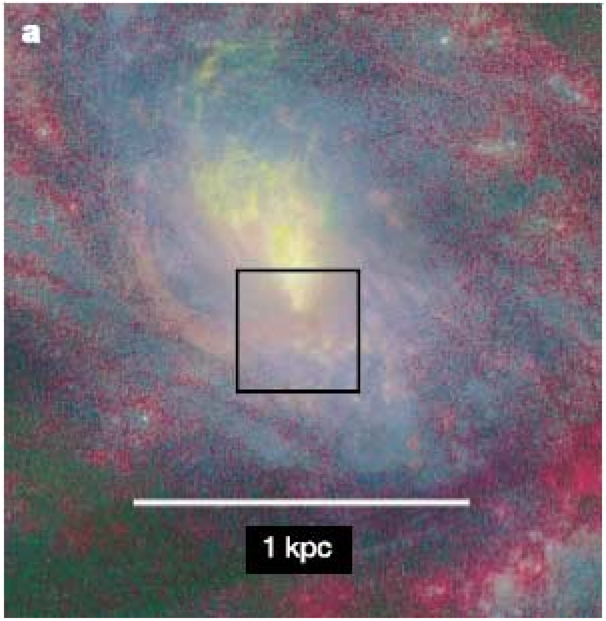

b, Single-telescope acquisition image (deconvolved) of NGC 1068 taken by MIDI with a 8.7 μm filter penetrating the dust and showing the structures on arcsec scales. These are similar to those of ref. 9. Also shown is the position of the spectroscopic slit used in the interferometric observations. The spectra displayed in Fig. 2 are integrated over the central emission peak only. The dashed line indicates the source axis. **c**, Model dust

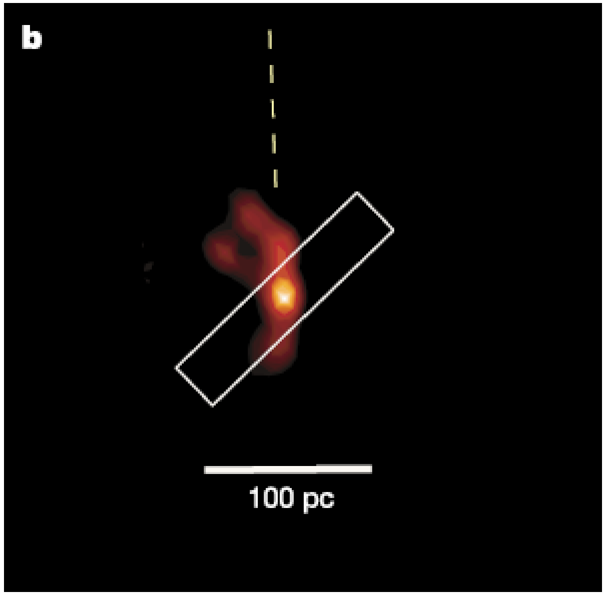

Figure 1 Images and model of emission from NGC 1068 at increasing magnification. **a**, Optical image of the central region of NGC 1068[20]. This colour composite taken with the Hubble Space Telescope shows stellar light in blue, oxygen ionized by the active nucleus in yellow and ionized hydrogen in red. The black square centred on the dust-obscured nucleus marks the region of **b**. In **a**–**c**, north is at the top, and east to the left.

Correlated flux and visibility

- While a single telescope sees all the flux within its field of view, a two-telescope interferometer sees only the flux on spatial scales smaller than the inverse of the telescope separation expressed in units of wavelength
- The correlated flux divided by the total flux is equal to the visibility amplitude

NGC 1068

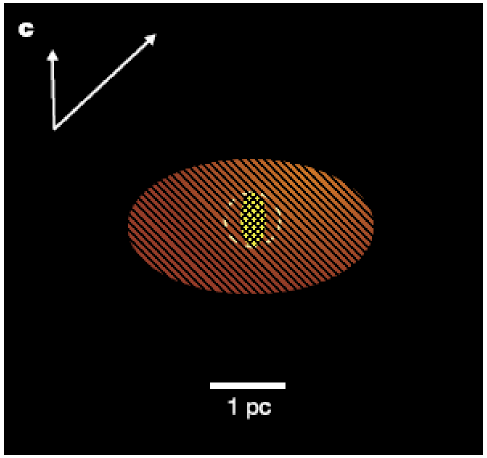

• Realize that MIDI is resolving a structure as fringe spacing decreases towards shorter wavelengths.
• Realize that the visibility increases at the shortest spacings: this indicates a second more compact emission (red line).
• Realize that the correlated flux is affected by the 10 μ dust absorption feature.
• Realize that the source spectra are blackbody, one 800 K (hot) and one 320 K (warm) component. The emission from both is absorbed by the dust.
• The dust opacity is an additional parameter to tweak the relative correlated fluxes.
• The shorter baseline at the largest fringe spacings resolves some large scale emission.

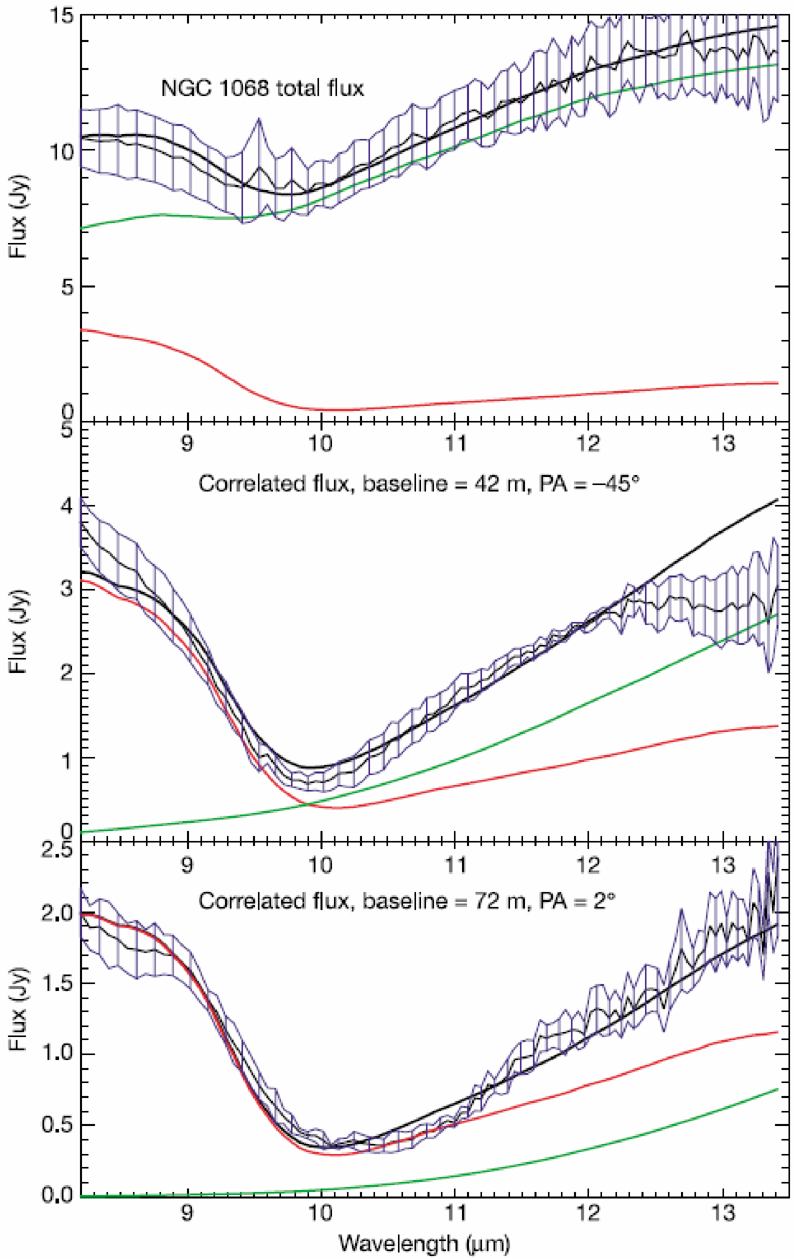

Jaffe et al. 2004

Two components

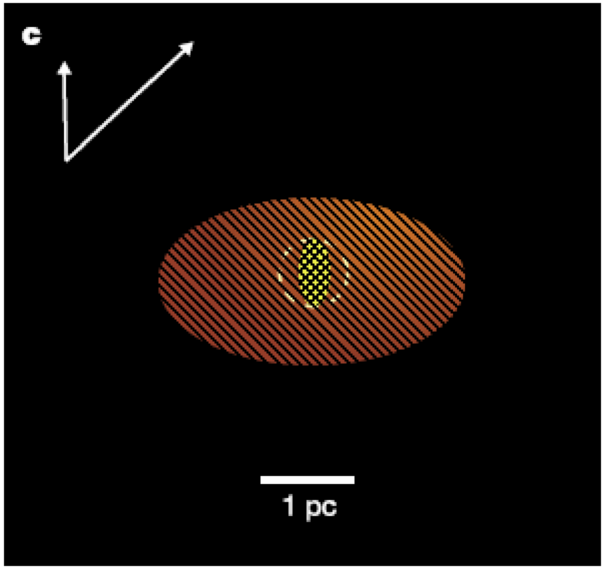

Table 1 **Dust emission components in the nucleus of NGC 1068**

Component	T (K)	$\Delta \parallel$ jet (mas)	$\Delta \parallel$ jet (pc)	$\Delta \perp$ jet (mas)	$\Delta \perp$ jet (pc)	τ_{SiO}
Hot	>800	10 ± 2	0.7 ± 0.2	<12	<1	2.1 ± 0.5
Warm	320 ± 30	30 ± 5	2.1 ± 0.4	49 ± 4	3.4 ± 0.3	0.3 ± 0.2

Each component is taken to be a two-dimensional gaussian aligned with one axis parallel to the radio jet. Sizes Δ are given as full-width at half-maximum of gaussian profiles. We have assumed emission from each component with a blackbody spectrum of the given temperature with constant emissivity. Emissivity decreasing rapidly with increasing wavelength ($\sim\lambda^{-1}$ or steeper), as might be expected from optically thin dust emission, is not consistent with the data. In front of this emission we impose an absorption of $\exp(-\tau(\lambda))$. $\tau(\lambda)$ varies with λ to match known silicate profiles as described in the text. The peak value of $\tau(\lambda)$ for each component is given here as τ_{SiO}. The optical depth τ in front of the hot component is in fact the sum of the contributions of the hot and warm components, because the model assumes that the absorption in the warm component also reduces the hot component. The errors refer to the full range of uncertainty when varying all parameters simultaneously. We assume the standard distance[21] of 14.4 Mpc (that is, 1 pc = 14.3 mas). The temperature of the hot component is a lower bound; the blackbody profiles from all temperatures above 800 K are indistinguishable within the observed wavelength band.

Not enough data?

Other sources of info:

- SED
- AO imaging
- Spectro-astrometry
- Other?

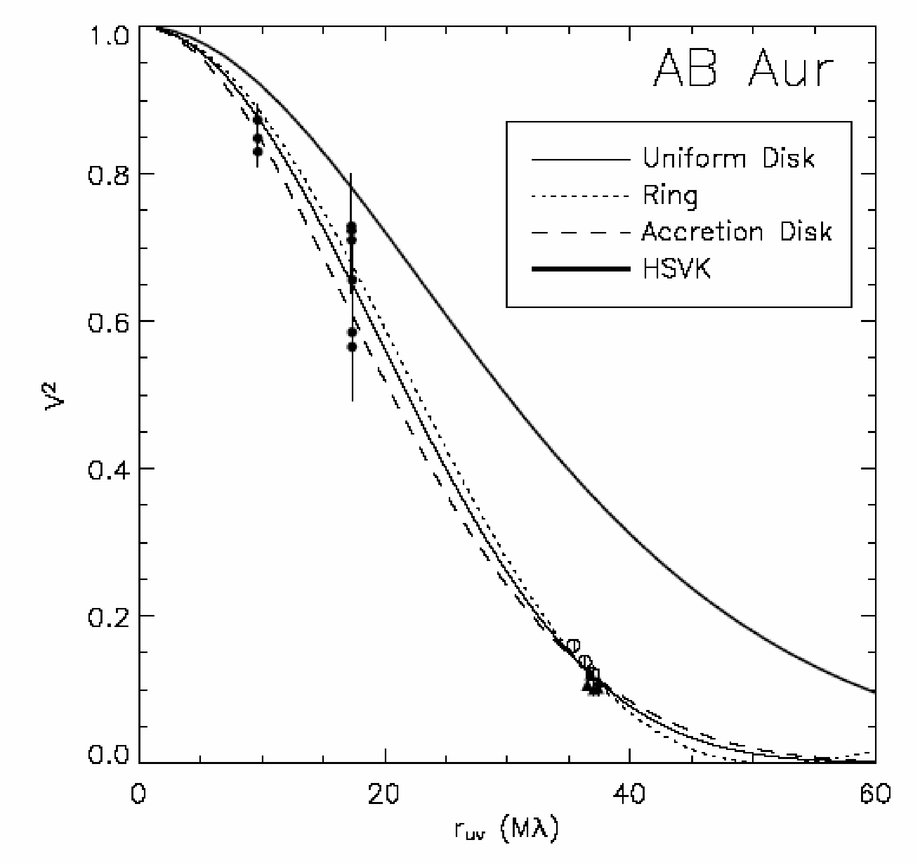

Eisner et al. 2003

Any questions?